JOURNAL OF APPLIED ELECTROCHEMISTRY 13 (1983) 253–267

Mineralogical and electrochemical stability of the nickel–iron sulphides—pentlandite and violarite

M. R. THORNBER

CSIRO, Division of Mineralogy, Wembley, Western Australia 6014, Australia

Received 6 April 1982

Mineralogical data on the oxidative weathering of primary nickel sulphide assemblages are used to calculate the thermodynamic stability fields for pentlandite ($(Fe, Ni)_9S_8$), violarite ($(Ni, Fe)_3S_4$), millerite (NiS), pyrite (FeS_2), pyrrhotite (Fe_7S_8), sulphur, sulphate and H_2S, as a function of pH, E_h, and the activities of Fe^{2+}, Ni^{2+} and S^{2-} in solution. This is compared with electrochemical experiments using cyclic voltammetry and intermittent galvanostatic polarization carried out on electrodes of pentlandite and violarite at pH values of 0, 2, 4, 6 and 8. The mechanisms of the cathodic and anodic reactions at the electrolyte/sulphide interface are postulated, and the similar behaviour of pentlandite and violarite is demonstrated. Below pH 4, anodic dissolution favours sulphur formation, and above pH 4 sulphate is formed. Cathodic dissolution favours H_2S formation over H_2 at low pH values. A method for hydrometallurgical dissolution of these minerals is suggested and a comprehensive description of pentlandite and violarite stability is presented.

1. Introduction

The mechanism of weathering of sulphide minerals in the geological environment, and the processes by which sulphides can be hydrometallurgically treated, are quite similar. Because most sulphides conduct electricity, they can be fashioned into electrodes and their interaction with aqueous solutions studied electrochemically in much the same way as metallic corrosion.

Extensive mineralogical and chemical studies have been made of the supergene weathering displayed by the nickel sulphide assemblages of Western Australia [1–3]. Pentlandite ($(Ni, Fe)_9S_8$) and violarite ($(Ni, Fe)_3S_4$) are generally the major nickel-containing minerals of these assemblages with only one shoot, the Otter at Kambalda, having significant millerite (NiS) as well as violarite [3]. Iron sulphide minerals, pyrrhotite (Fe_7S_8) and pyrite (FeS_2) are also major constituents. Copper minerals are among the many other minor constituents that will be ignored in this discussion, mainly for the sake of simplicity.

The common methodology is to make mineralogical observations and then use thermodynamic calculations to show that the mineralogical interpretations are valid. This approach breaks down where the reactions that are being considered involve the alteration of crystalline materials at temperatures below 323 K, i.e. weathering reactions. Free energies of formation (ΔG_f) of solids are usually measured at high temperatures where it is reasonable to assume that equilibrium has been reached. These ΔG_f values are then extrapolated down to standard temperature, and this assumes usually that there is no entropy change in the components and the solid products of the formation reaction, i.e., that there are no changes of atomic arrangement, bonding electron behaviour or magnetic interactions etc. in the extrapolated temperature range. Thermodynamic data estimated from room temperature electrochemical studies are not reliable either, as modern electrochemical theory has shown that conditions at the interface between a solid and an electrolyte cannot be explained by application of the thermodynamic Nernst equation [4] as most electrode reactions are not at equilibrium.

The purpose of this paper is to show how mineralogical observations can be used in conjunction with

0021–891X/83/020253–15$04.30/0

electrochemical measurements to give a more reliable set of parameters for describing the low-temperature stabilities of the economically important nickel-iron sulphide minerals.

2. Experimental procedure

2.1. *Preparation of electrodes*

Synthetic violarite was prepared by the method of Craig [5]. Many attempts to synthesize pure pentlandite by annealing mixtures of pure Fe and Ni metals with the appropriate amount of S in evacuated quartz tubes, all produced trace amounts of a hexagonal monosulphide solid-solution phase closely intermixed with the pentlandite. A nearly pure natural pentlandite from Nepean in Western Australia was therefore used. This pentlandite was finely ground, so that the slight pyrrhotite contamination could be leached out with concentrated hydrochloric acid. The electrodes were prepared under N_2 by packing fine powders of the appropriate sulphide minerals into gold tubes which were evacuated and sealed. These were heated to 623 K under hydrostatic pressure in a bomb apparatus for two days. The gold tubes were cut in half, and part of the gold peeled off from the middle. Copper wire was soldered to the remaining gold to make good electrical contact with the sulphide. The sulphide pellets were then mounted end-on in epoxy resin to give an exposure of sulphide mineral that could be polished for mineralogical examination. A cross section of such an electrode is shown in Fig. 1a. The violarite electrodes produced in this way were well compacted, and single phase of uniform composition. If the pentlandite face still showed the slightest trace of pyrrhotite, this was then leached out with hydrochloric acid. In order to preserve the pentlandite, the electrode was made cathodic in the acid so that the dissolution of pyrrhotite as a cathodic reaction

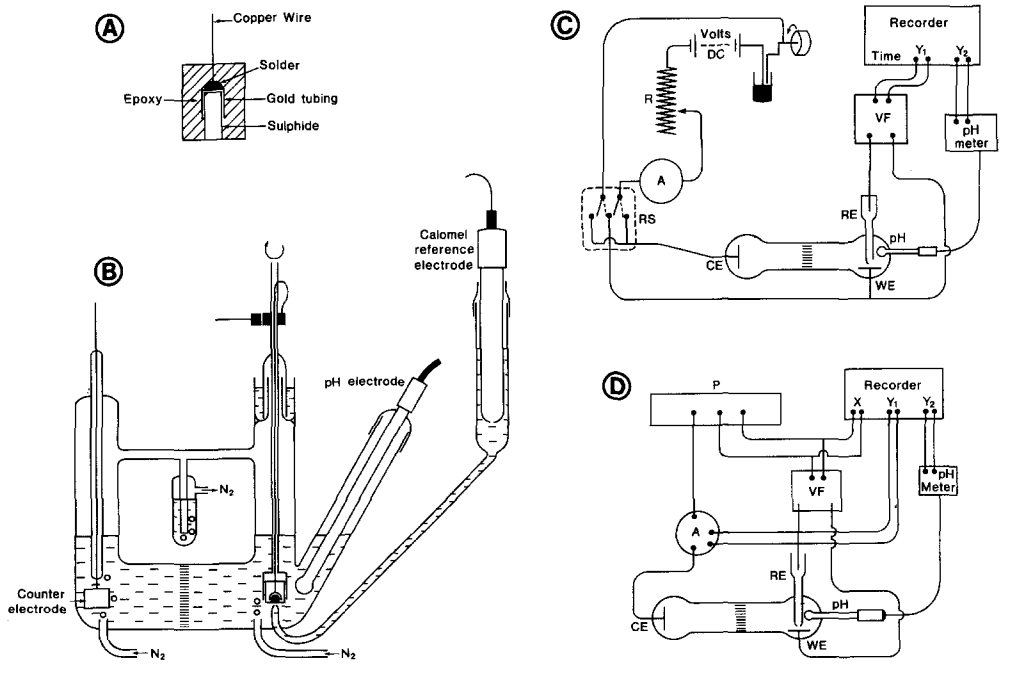

Fig. 1. Schematic diagram of the test cell and circuits. (a) cross section of the mineral electrode. (b) test cell. (c) intermittent galvanostatic potential circuit. (d) cyclic voltammetry circuit. RE = reference electrode; WE = working electrode; CE = counter electrode; RS = reversing switch; VF = voltage follower; P = potentiostat; R = resistance.

$$Fe_7S_8 + 16H^+ + 2e^- \rightarrow 8H_2S + 7Fe^{2+}$$

would be favoured over the anodic dissolution of pentlandite

$$Fe_{4.5}Ni_{4.5}S_8 + 16H^+ \rightarrow 8H_2S + 4.5Fe^{2+} + 4.5Ni^{2+} + 2e^-$$

The surface of the electrode was then re-impregnated with epoxy and polished back to give a surface that was exclusively pentlandite.

These electrodes were studied by two more or less complementary electrochemical techniques mainly as a cross check to establish what was a reproducible reaction of the mineral electrode. The same reaction cell was used for both techniques, and is shown diagrammatically in Fig. 1b. The cell was purged with high-purity water saturated nitrogen gas, and a constant excess pressure of nitrogen was maintained during experimentation by continually passing N_2 through the counter-electrode side of the chamber. The electrolytes used were 0.1 mol dm^{-3} NaCl and $NaNO_3$ solutions. $NiCl_2$ was also included in the solution for some experiments. The pH was adjusted with HCl or HNO_3 where appropriate.

2.2. *Intermittent galvanostatic polarization (IGP) method [6].*

The circuit used for this technique is shown in Fig. 1c. One-second pulses of current were passed through the electrode surface at one-second intervals, and the potential between the sulphide electrode and reference electrode was recorded as a function of time, as shown in Figs. 2 and 3. The current was supplied from a D.C. battery source at 45 or 90 V, and the swamping resistor R was adjusted to give the required constant current. The direction of the current was usually reversed several times during a particular experiment, so that where the potential is more positive than the rest potential an anodic current is flowing and where the potential has dropped suddenly to be more negative than the rest potential the current has been reversed and a cathodic current is flowing (Figs. 2 and 3). The experiment was first run at the lowest current possible (0.01 mA cm^{-2}) and, after completing several cycles with the current flowing both cathodically and anodically, the current was increased to a new value and the procedure was repeated. In this way the electrode was subjected to increasing current and thus increasing reaction rates. Figs. 2 and 3 show reactions at currents of 0.01, 0.1, 1.0 and 8 mA cm^{-2} at pH values of 0, 2, 4, 6 and 8 for pentlandite and violarite, respectively. At pH values of 4, 6 and 8 the reactions significantly altered the pH, and this pH variation, as well as the potential change, was monitored by means of a 2-pen recorder coupled to a pH meter and electrode (see Fig. 1c). The pH electrode response was subject to interference from the current flowing between the working electrode and the counter electrode. The extent of this can be seen in the thickness of pH lines, shown in Figs. 2 and 3, which indicates the pH response for current on and off. The electrode responded well to relative changes in pH, however while larger currents were flowing the absolute pH was in error by as much as 0.1. Additional IGP traces were made for a more complete series of current values than those shown in Figs. 2 and 3, and all of these have been correlated to give the comparison between current flow and potential shown in Fig. 4.

2.3. *Cyclic voltammetry*

The electrical circuit shown in Fig. 1d employed a potentiostat that controlled the potential of the sulphide electrode, and the current flow was recorded as a function of the potential. The potentiostat was motor driven so that the potential of the electrode could be continuously changed at either 67 mV s^{-1} or 6.7 mV s^{-1}. The potential sweeps at 6.7 mV s^{-1} at pH values of 0, 2, 4 and around 6 are shown in Fig. 5 for violarite and pentlandite. At pH 4 and 6 the pH was also monitored, as the reactions also affected the pH. This gave a recording of pH variations in the bulk of the solution and can only be used as a clue to the interfacial pH.

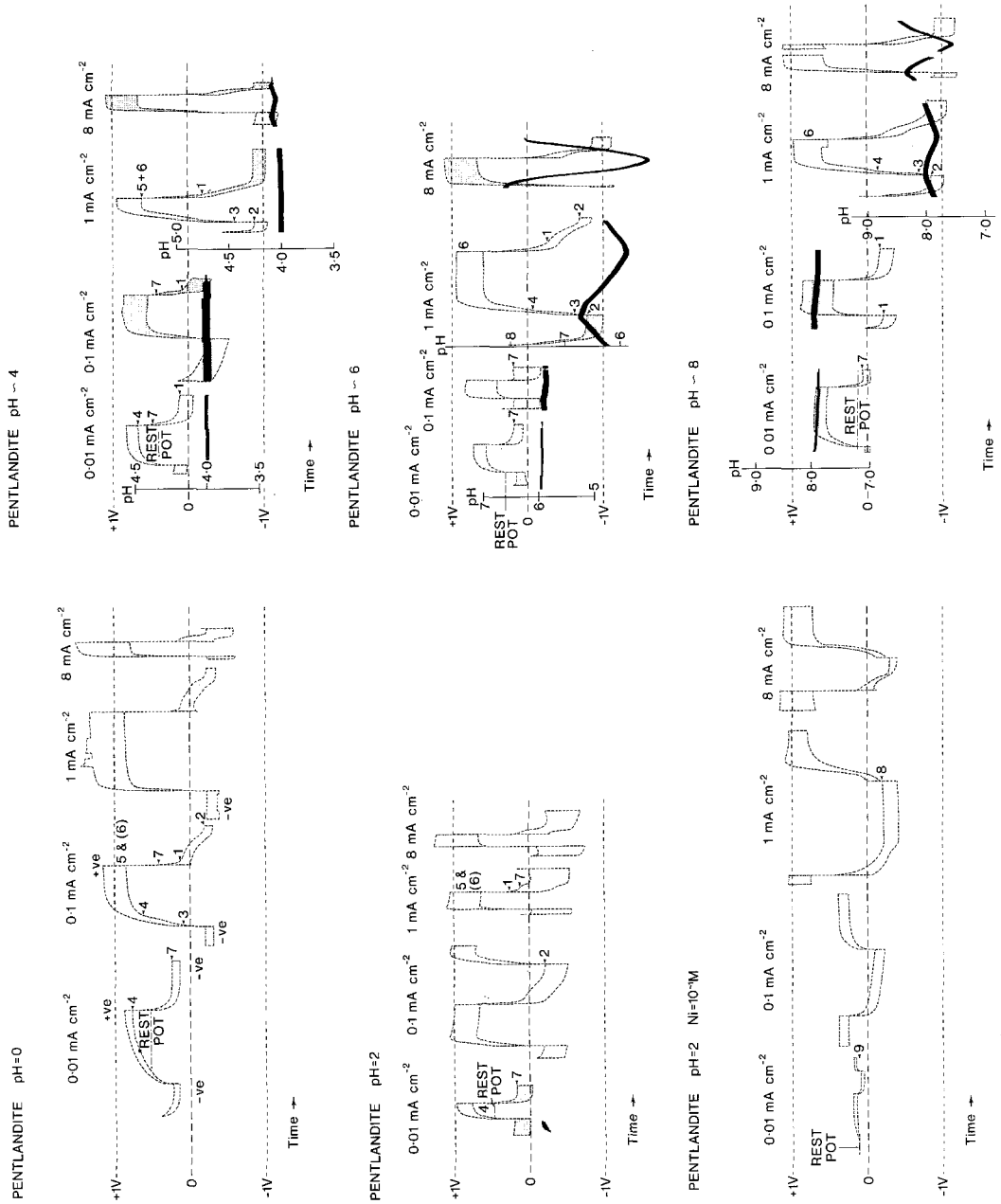

Fig. 2. IGP traces for pentlandite at pH 0, 2, 4, 6 and 8 in 0.1 mol dm^{-3} NaCl and the appropriate addition of HCl. A trace is also shown at pH 2 where 0.1 mol dm^{-3} Ni^{2+} was also in the electrolyte. Numbers on the traces refer to the reactions of Fig. 7. Heavy lines show the pH variation. The area between the dashed lines represents the potential covered between the current-on for 1 s and the current-off for 1 s.

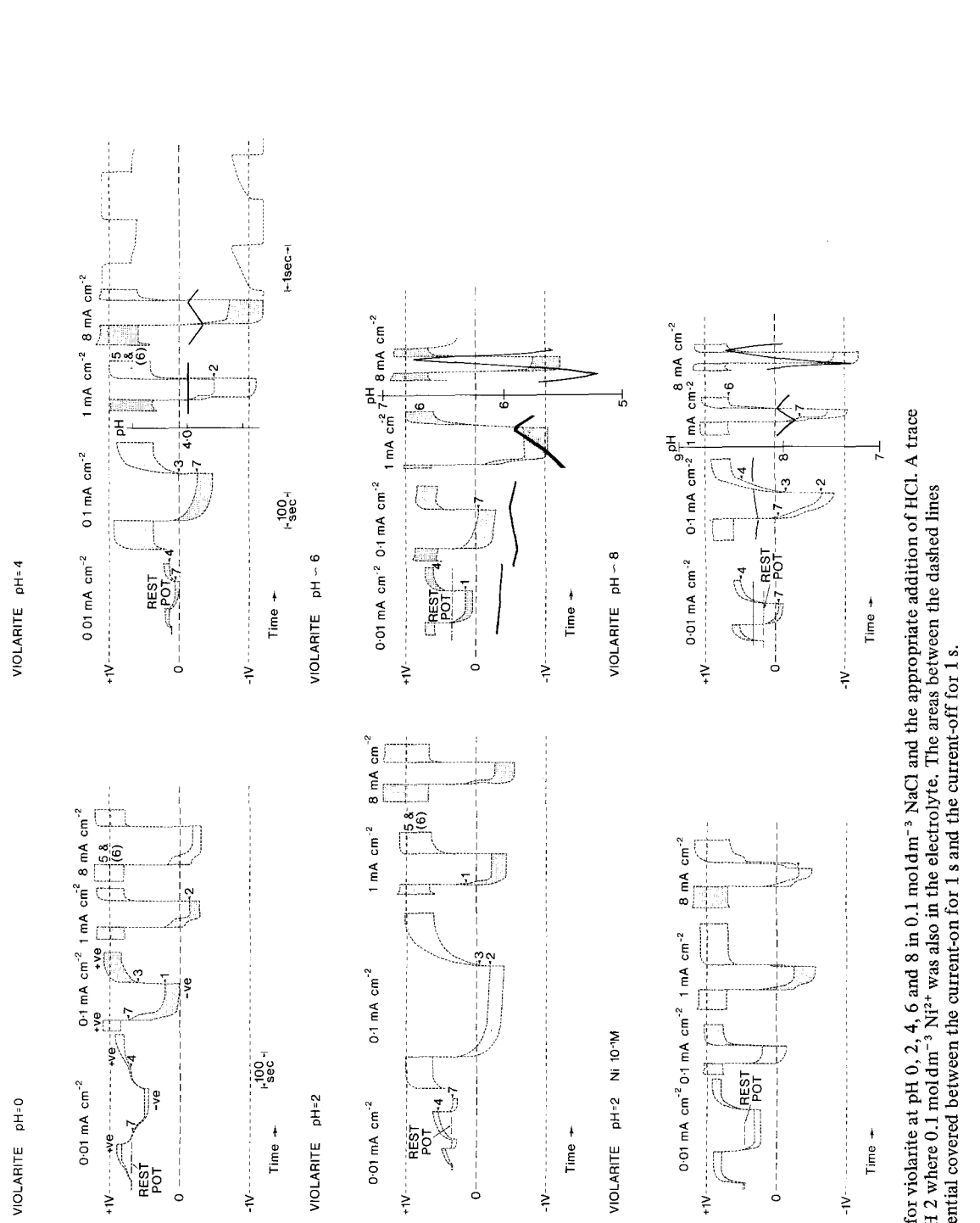

Fig. 3. IGP traces for violarite at pH 0, 2, 4, 6 and 8 in 0.1 mol dm^{-3} NaCl and the appropriate addition of HCl. A trace is also shown at pH 2 where 0.1 mol dm^{-3} Ni^{2+} was also in the electrolyte. The areas between the dashed lines represents the potential covered between the current-on for 1 s and the current-off for 1 s.

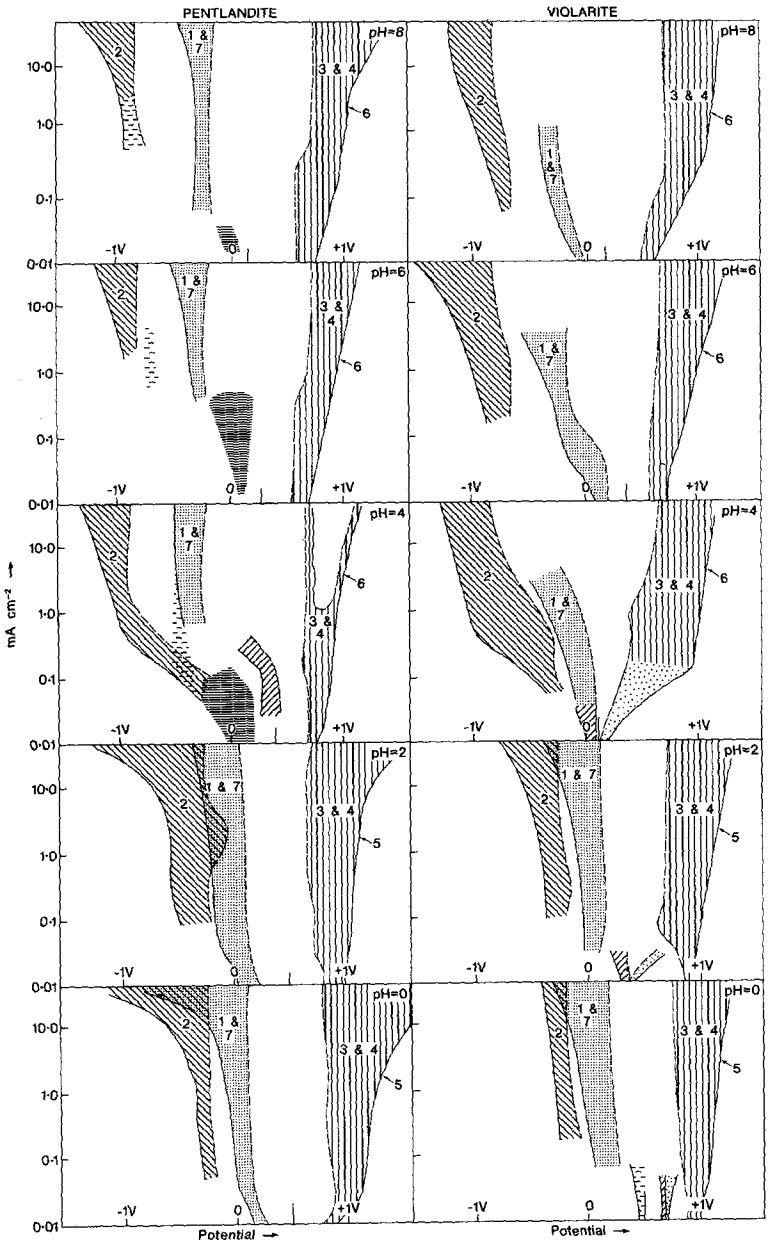

Fig. 4. Compilation of the combined IGP data for both pentlandite and violarite showing the relationship between current flow and potential. The solid lines represent the current-on potential for the particular reaction and the dashed lines the current-off potential. The numbers refer to the reactions shown in Fig. 7.

3. Results

3.1. *Mineralogical observations and thermodynamic calculations*

The mineralogical and chemical studies on the supergene weathering of the nickel iron sulphides of Western Australia are well documented [1–3, 7, 8] and the reactions listed in Table 1 result from these studies. The observed reactions are what have taken place over tens of millions of years and represent, as nearly as possible, the stable phase relations. In Table 1, fixed formulae are given for pentlandite, violarite and pyrrhotite, to keep the thermodynamic diagrams as simple as possible. In practice the Ni : Fe ratio varies in pentlandite from 1:1 up to 1.5 : 1 while that of violarite can vary from 1:1 through to the

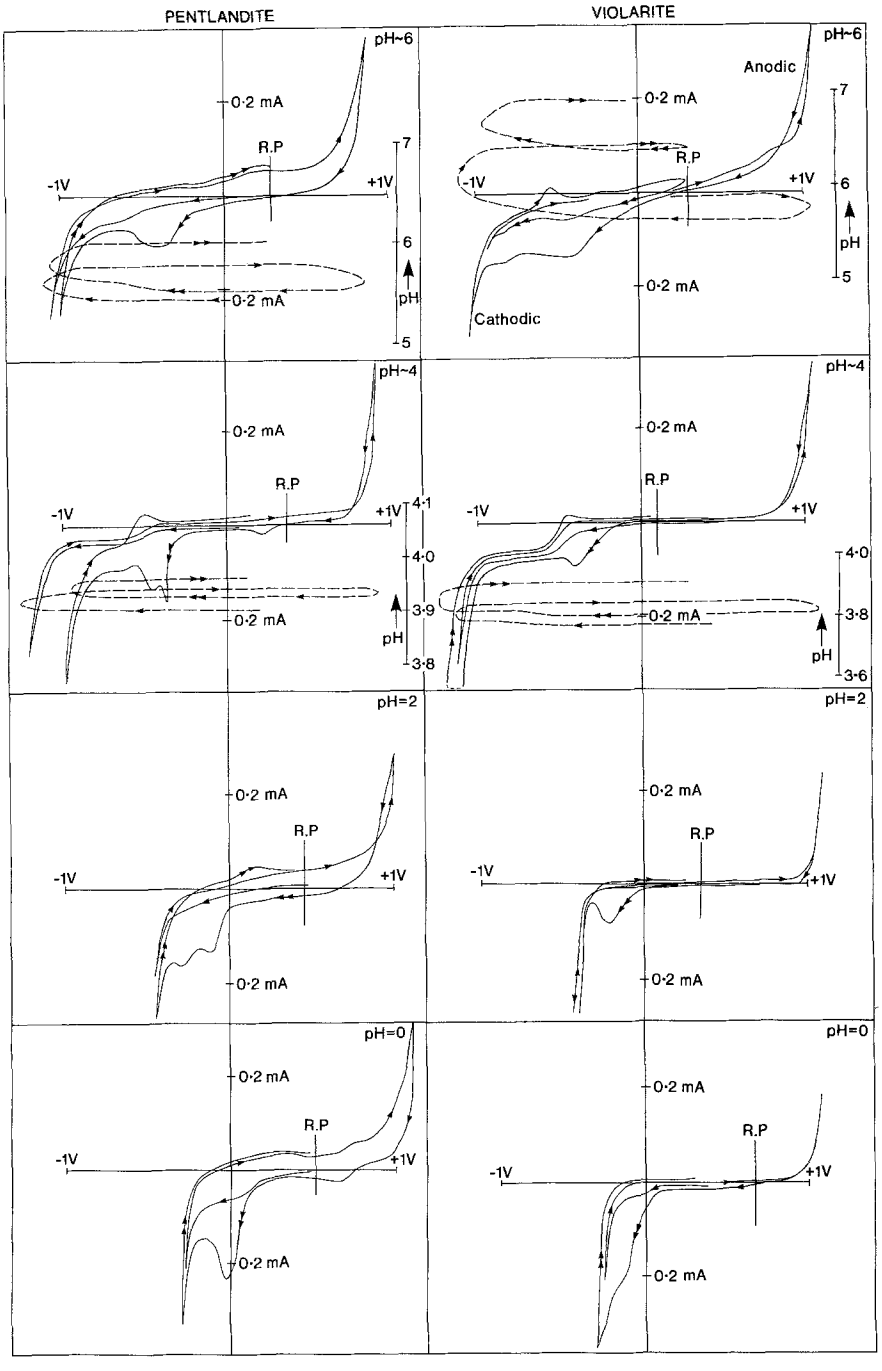

Fig. 5. Cyclic voltammograms of pentlandite and violarite in 0.1 mol dm^{-3} NaCl and various pH values. Solid lines indicate current; dashed lines, pH.

all nickel end member Ni_3S_4 polydymite [1, 3, 5]. The Fe : S ratio of pyrrhotite can vary from the FeS of troilite through to the Fe_7S_8 of monoclinic pyrrhotite which is used here.

In summary, in a primary mineral assemblage composed of pentlandite, pyrrhotite and pyrite, pentlandite reacts first at the lowest oxidation potential by being altered to violarite, with nickel and iron being released into solution, as in Equation (a), Table 1. At the same time, the increased nickel activity

Table 1. Reactions and thermodynamic equations

(a) Pentlandite Violarite
$Fe_{4.5}Ni_{4.5}S_8 \rightarrow 2FeNi_2S_4 + 0.5Ni^{2+} + 2.5Fe^{2+} + 6e^-$
$E_h = -0.2354 + 0.0049 \log[Ni^{2+}] + 0.0247 \log[Fe^{2+}]$

(b) Pentlandite m-Pyrrhotite
$Fe_{4.5}Ni_{4.5}S_8 + 2.5Fe^{2+} \rightarrow Fe_7S_8 + 4.5\,Ni^{2+} + 4e^-$
$E_h = 0.0561 - 0.0370 \log[Fe^{2+}] + 0.0665 \log[Ni^{2+}]$

(c) m-Pyrrhotite Violarite
$Fe_7S_8 + 4Ni^{2+} \rightarrow 2FeNi_2S_4 + 5Fe^{2+} + 2e^-$
$E_h = -0.8185 - 0.1183 \log[Ni^{2+}] + 0.1478 \log[Fe^{2+}]$

(d) Pentlandite Millerite
$Fe_{4.5}Ni_{4.5}S_8 + 3.5Ni^{2+} \rightarrow 8NiS + 4.5Fe^{2+} + 2e^-$
$E_h = -0.2748 - 0.1035 \log[Ni^{2+}] + 0.1331 \log[Fe^{2+}]$

(e) Millerite Violarite
$4NiS + Fe^{2+} \rightarrow FeNi_2S_4 + 2Ni^{2+} + 2e^-$
$E_h = -0.2157 + 0.0592 \log[Ni^{2+}] - 0.0296 \log[Fe^{2+}]$

(f) Violarite Pyrite
$FeNi_2S_4 + Fe^{2+} \rightarrow 2FeS_2 + 2Ni^{2+} + 2e^-$
$E_h = +0.0748 + 0.0592 \log[Ni^{2+}] - 0.0296 \log[Fe^{2+}]$

(g) m-Pyrrhotite Pyrite
$Fe_7S_8 \rightarrow 4FeS_2 + 3Fe^{2+} + 6e^-$
$E_h = -0.223 + 0.296 \log[Fe^{2+}]$

(h) Pyrite
$FeS_2 \rightarrow 2S + Fe^{2+} + 2e^-$
$E_h = 0.4217 + 0.0296 \log[Fe^{2+}]$

(i) Pentlandite
$Fe_{4.5}Ni_{4.5}S_8 + 16H^+ \rightarrow 4.5Ni^{2+} + 4.5Fe^{2+} + 8H_2S + 2e^-$
$E_h = -0.0250 + 0.4733pH + 0.1331 \log[Ni^{2+}] + 0.1331 \log[Fe^{2+}] + 0.2366 \log[H_2S]$

(j) Violarite
$Fe^{2+} + 2Ni^{2+} + 4H_2S \rightarrow FeNi_2S_4 + 8H^+ + 2e^-$
$E_h = -0.3406 - 0.2366pH - 0.1183 \log[H_2S] - 0.0592 \log[Ni^{2+}] - 0.0296 \log[Fe^{2+}]$

(k) m-Pyrrhotite
$7Fe^{2+} + 8H_2S \rightarrow 16H^+ + Fe_7S_8 + 2e^-$
$E_h = 0.1177 - 0.4733pH - 0.2071 \log[Fe^{2+}] - 0.2366 \log[H_2S]$

(l) Millerite
$NiS + 2H^+ \rightarrow H_2S + Ni^{2+}$
$E_h = -1.0555 - \log[H_2S] + \log[Ni^{2+}] + 2pH$

(m) Pyrite
$2H_2S + Fe^{2+} \rightarrow FeS_2 + 4H^+ + 2e^-$
$E_h = -0.1379 - 0.1183pH - 0.0296 \log[Fe^{2+}] - 0.0592 \log[H_2S]$

(n) Violarite
$FeNi_2S_4 + 16H_2O \rightarrow Fe^{2+} + 2Ni^{2+} + 4SO_4^{2-} + 32H^+ + 30e^-$
$E_h = 0.3433 + 0.0039 \log[Ni^{2+}] + 0.00197 \log[Fe^{2+}] + 0.0079 \log[SO_4^{2-}] - 0.063pH$

(o) Millerite
$NiS + 4H_2O \rightarrow Ni^{2+} + SO_4^{2-} + 8H^+ + 8e^-$
$E_h = 0.3083 + 0.0074 \log[Ni^{2+}] + 0.0074 \log[SO_4^{2-}] - 0.0592pH$

(p) Pyrite
$FeS_2 + 8H_2O \rightarrow Fe^{2+} + 2SO_4^{2+} + 16H^+ + 14e^-$
$E_h = 0.3624 - 0.0676pH + 0.00423 \log[Fe^{2+}] + 0.00845 \log[SO_4^{2-}]$

(q) $S + 4H_2O \rightarrow SO_4^{2-} + 8H^+ + 6e^-$
$E_h = 0.3526 + 0.00986 \log[SO_4^{2-}] - 0.0788pH$

(r) Pentlandite
$Fe_{4.5}Ni_{4.5}S_8 + 32H_2O \rightarrow 4.5Fe^{2+} + 4.5Ni^{2+} + 8SO_4^{2-} + 64H^+ + 66e^-$
$E_h = 0.2907 + 0.00403 \log[Fe^{2+}] + 0.00403 \log[Ni^{2+}] + 0.00717 \log[SO_4^{2-}] - 0.05733pH$

Table 2. Free energy of formation data

Compound	*Formula*	ΔG_f kJ mol^{-1}	*Reference*
violarite	$FeNi_2S_4$	− 18.2	[10]
		− 19.9	adjusted value
pentlandite	$Fe_{4.5}Ni_{4.5}S_4$	− 47.8	[10]
		− 44.5	adjusted value
pyrite	FeS_2	− 9.2	[11]
millerite	NiS	− 4.5	[12]
m-pyrrhotite	Fe_7S_8	− 42.8	[12]
sulphur	S	0	[12]
hydrogen sulphide	H_2S (aq)	− 1.6	[12]
sulphate	SO_4^{2-}	− 42.6	[12]
water	H_2O	− 13.6	[12]
hydrogen ion	H^+	0	[12]
ferrous ion	Fe^{2+}	− 4.5	[12]
nickel ion	Ni^{2+}	− 2.6	[12]

causes the pyrrhotite to become unstable and it takes up nickel from solution to form violarite, as in Equation (c). The pyrite, meanwhile, is unaffected. This process continues until all of the pentlandite is altered to violarite, and then, at a higher oxidation potential, any remaining pyrrhotite alters to pyrite (Equation (g)) until the pyrrhotite is completely consumed and the supergene assemblage of violarite + pyrite is formed. At still higher oxidation potentials, these secondary sulphides oxidize further, with nickel going into solution and sulphate being formed (Equations (n) and (p)).

The other type of primary assemblage is that of the Otter Shoot at Kambalda [3] and consists of a primary pentlandite–millerite–pyrite assemblage where the pentlandite has a higher Ni : Fe ratio than the pentlandite from a pentlandite–pyrrhotite–pyrite assemblage. This nickel-rich pentlandite undergoes an oxidation reaction to produce a more nickel-rich violarite; however the reaction is essentially the same as reaction (a). The millerite is then observed to undergo oxidation to a nickel-rich violarite, and this reaction also involves the uptake of some iron, as shown by the generalized reaction (e). Thus, a violarite–pyrite supergene assemblage is formed and, although it contains more nickel than that formed from the pentlandite–pyrrhotite assemblage, it still undergoes further oxidation in the same way by the reactions (n) and (p).

The equations relating E_h, pH and the various activities of components were calculated in the usual manner [9] using the data listed in Table 2. Initial calculations carried out using Graig and Naldrett's [10] values for the free energy of formation (ΔG_f) at 298 K for pentlandite and violarite came up with the result that violarite does not exist and that, under all conditions, pyrrhotite, pentlandite and millerite would always weather to either pyrite or to sulphate in solution. However, the mineralogical observations show that all of these minerals can oxidize to violarite. It could be argued that the violarite is a metastable intermediate, but it is much easier to accept that the thermodynamic data are wrong for these lower temperatures, and that the ΔG_f data of pentlandite and violarite should be adjusted so that the thermodynamic calculations are made to fit the mineralogical observations. Craig and Naldrett [10] measured the thermodynamic data for pentlandite and violarite at temperatures from 1373 K down to 573 K, and the calculations of ΔG_f at 298 K involved the assumption that there are no entropy changes for the formation reactions between 573 and 298 K. Natural pentlandite undergoes a crystal transformation between 323 K and 473 K [13]; violarite has not been studied so extensively, but pyrrhotite [14, 15] undergoes crystal and magnetic ordering at low temperatures. For these reasons it may be too much to expect reliable values for the free energies of formation of sulphide minerals at temperatures extrapolated below 473 K. The data listed in Table 1 are a self-consistent set that was calculated and selected, using ΔG_f at 298 K of pyrite [11] as an anchor value, so that the set conforms with the miner-

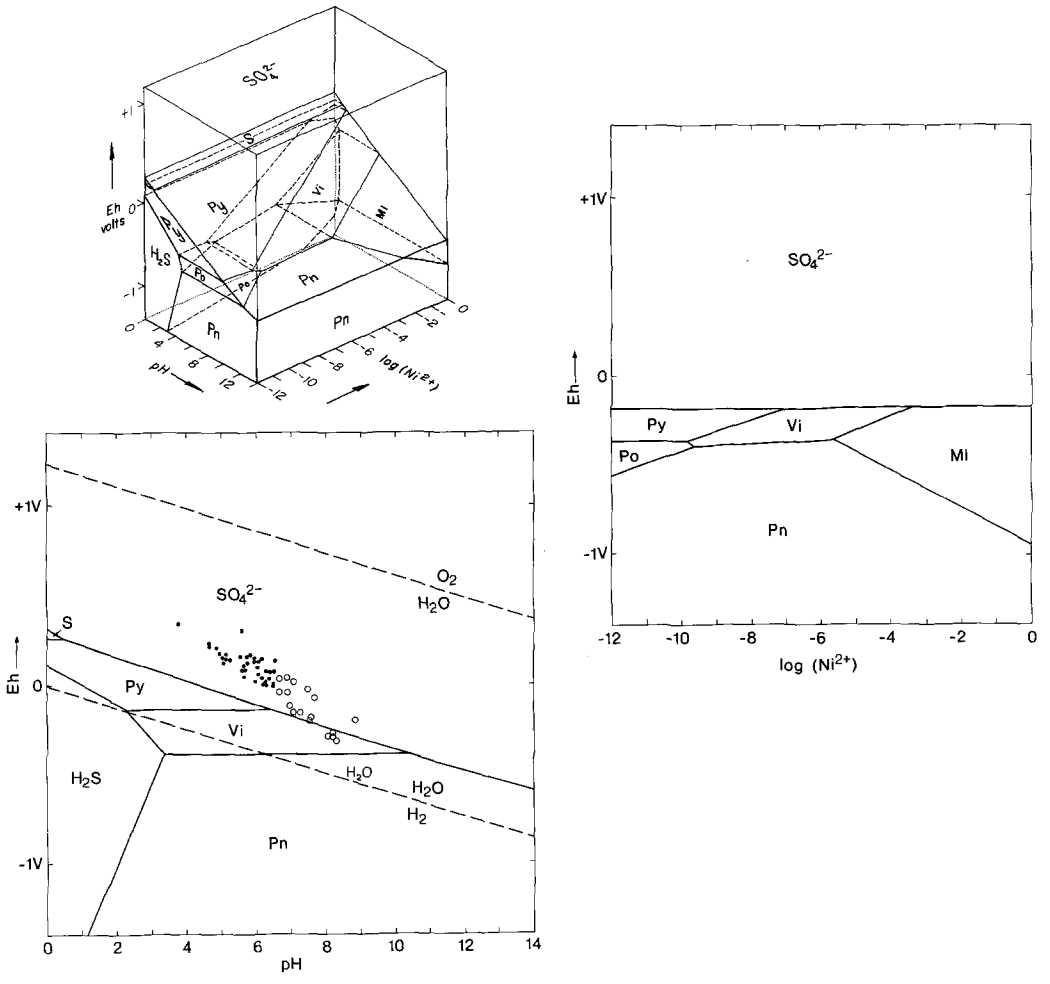

Fig. 6. E_h–pH–Activity diagrams at 298° C drawn from data listed in Tables 1 and 2. Activities of Fe^{2+}, SO_4^{2-} and Ni^{2+}, where constant, are taken to be 10^{-6}, and H_2S activity is assumed to be 10^{-2}. Py = pyrite, Pn = pentlandite, Vi = violarite, Ml = millerite, Po = pyrrhotite. (a) Three-dimensional E_h–pH–log[Ni^{2+}] diagram. (b) E_h–log(Ni^{2+}) section at pH = 7. (c) E_h–pH section where (Ni^{2+}) = 10^{-6}. Data points are E_h–pH measurements made on pentlandite–violarite assemblages [8].

alogical observations. The E_h–pH–activity diagrams of Fig. 6a, b and c were calculated from these data. The areas on these diagrams where SO_4^{2-} is shown is where metal oxides and oxyhydroxides are stable.

3.2. *Results of electrochemical experiments*

The reactivities of pentlandite and violarite were studied electrochemically, and the results are compared with the thermodynamic representation of the mineralogical observations.

Cyclic voltammetry traces for pentlandite and violarite are shown in Fig. 5 at pH 0, 2, 4, and varying from 5–7; they were carried out in 0.1 mol dm^{-3} NaCl solution and repeated in 0.1 mol dm^{-3} $NaNO_3$ solution, which gave essentially similar traces. The NaCl solution was used to give greater similarity to a natural ground-water system than $NaNO_3$ solution.

To supplement the cyclic voltammetry data, the intermittent galvanostatic polarization (IGP) method of Horvarth and Hackl [6] was also used, and the traces produced for both pentlandite and violarite are shown in Figs. 2 and 3. Here traces are shown with both positive and negative current flowing inter-

mittently at one-second intervals, at traces of 0.01 mA cm^{-2}, 0.1 mA cm^{-2}, 1 mA cm^{-2} and 8 mA cm^{-2}, at pH values of 0, 2, 4, around 6 and around 8. At pH of 4, 6 and 8 the pH change was also monitored and is also shown. In Fig. 3, violarite at pH 4 also shows the shape of two typical on/off traces at a faster recorder time base. By the IGP method, the off part of the reaction band gives an indication of the potential of the sulphide surface when no externally imposed current is flowing, and thus the potential at which a particular reaction is initiated can be better estimated.

Reactions that are taking place at the mineral surface can be postulated by a variety of methods, including chemical analysis of the solutions, watching the surface for the appearance of gas bubbles, sniffing for the smell of H_2S, and examination of the mineral electrode surface, by electron microprobe analyser/scanning electron microscope. Undoubtedly complex adsorption and hydrolysis reactions take

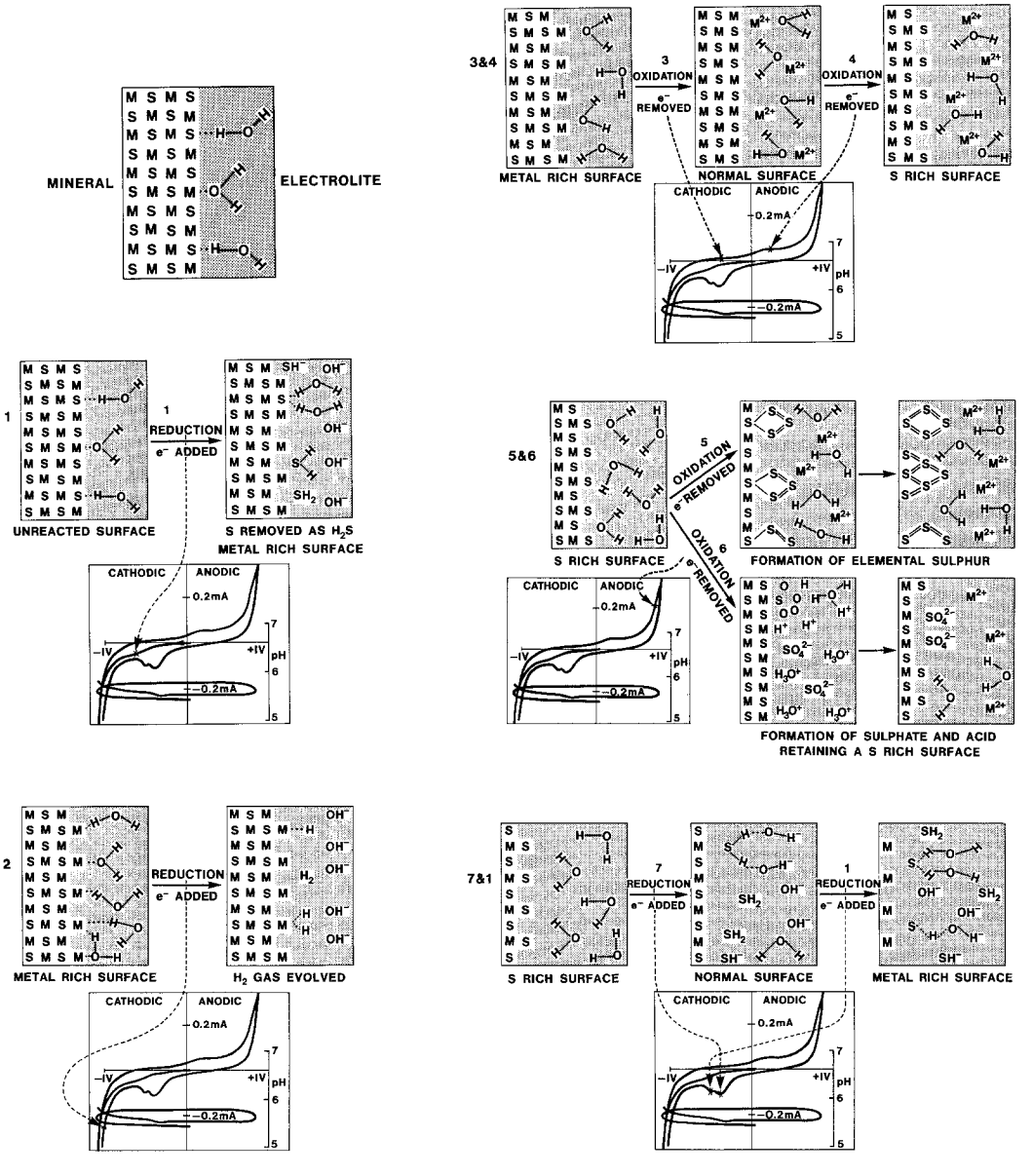

Fig. 7. Hypothetical representation of a section through a pentlandite or violarite surface – electrolyte interface as it reacts during a cathodic–anodic potential cycle. Reaction numbers correlate with those used in Figs. 2, 3 and 4.

place within the solution but the evidence from the rate of acid production, examination of the electrode surfaces and chemical analysis of the final solutions is that the actual reactions being forced on the mineral electrolyte interface does not involve the formation of metal hydroxides as is discussed later. However at the higher pH values some hydrolysis of metals would be expected. In Fig. 4 the vertically delineated reaction marked 3 and 4, at pH 6 and 8 for pentlandite, there are two constant potential steps relative to current density where no imposed current is flowing (i.e. the dotted line). This is due to some change in the surface of the pentlandite that could be associated with hydrolysis of metals. The other reactions shown in Fig. 4 at low current densities and with different hatchings are likely to be due to adsorption. The proposed hypotheses are directed more towards the reactions of the mineral component at the interface. These reactions are represented schematically in Fig. 7 in relation to a typical cyclic voltammetry trace for either pentlandite or violarite. In Fig. 7 the potential at which the particular surface reaction takes place is pointed out by the dotted arrows directed towards the cyclic voltammetry trace. The same reaction numbers are shown adjacent to potentials for those reactions of the IGP traces of Figs. 2, 3 and the combined diagrams of Fig. 4.

As shown in Fig. 7, reaction 1, the sequence of proposed reactions begins with the ideal unreacted sulphide/electrolyte interface, being reduced to a metal-rich surface as sulphide is dissolved to give H_2S and an increase in pH. The main evidence for this is the production of gas bubbles associated with the increase in pH and the smell of H_2S at the potential of this reaction. Some chemisorption of hydrogen probably also takes place at these potentials. Figure 7, reaction 2 shows how the metal-rich surface allows the water to be reduced to hydrogen gas, some hydrogen also being adsorbed onto the surface. Quantitative measurement of the rate of pH increase has shown that one OH^- is produced for each electron passed, which corresponds to the reaction:

$$2H_2O + 2e^- \rightarrow H_2\uparrow + 2OH^-.$$

On the positive sweep, reactions 3 and 4 (Fig. 7) show how metals on and in the surface are oxidized into solution to leave the surface sulphur-rich. This is based mainly on the evidence that changing the potential back to cathodic, subsequent to these reactions, still generates H_2S, indicating that a sulphur-rich surface must have been formed. Fig. 7, reaction 5 represents how sulphur enrichment can be carried further to give a porous elemental sulphur-coated surface if the pH is low enough (< 4). Progressively more metal is leached into solution, and dissolution through the sulphur layer forming on the surface probably limits the reaction rate. The sulphur forming on the mineral surface was verified by electron microprobe analysis of the mineral electrode surface. Count rates for sulphur were greatly enhanced over those for nickel and iron as compared with an unreacted surface. Material scraped from the electrode surface gave a diffuse powder X-ray pattern of rhombic sulphur. This reaction does not alter the pH unless the dissolved metal ions begin to hydrolyse. At pH values above 4 the sulphur also undergoes oxidation to sulphate, as indicated by reaction 6 in Fig. 7. Figures 2, 3 and 5 show how this reaction produces acid. Careful measurement of the rate of acid production during the IGP runs showed that there was one H^+ being produced for each electron flowing to within an error of less than ± 0.1. This is consistent with reactions (n) and (r), as listed in Table 1, taking place. If there was hydrolysis of metals as well then 1.25 H^+ should be produced per electron flowing. Chemical analysis of the solutions by atomic adsorption techniques for Ni, Fe and SO_4^{2-} (addition of excess Ba^{2+}) gave results consistent with only reactions (n) or (r) occurring. Figure 8 shows how, for pentlandite, violarite and millerite, this reaction will proceed at a progressively greater current, producing increasing acid until reaction 5 gradually takes over, there is no further decrease in pH, and the current flow becomes constant.

These reactions leave the surface rich in sulphur, and a cathodic sweep produces H_2S by reactions 7 and 1, as shown in Fig. 7.

Figures 2 and 3 show a comparison of IGP traces at pH 2 with and without 10^{-1} mol dm^{-3} Ni^{2+} in solution, for pentlandite and violarite, respectively. The pentlandite shows adsorbed Ni^{2+} affecting the rest potential with a reversible reaction at low current densities, and both pentlandite and violarite show reversible plating of nickel metal at higher cathodic current densities.

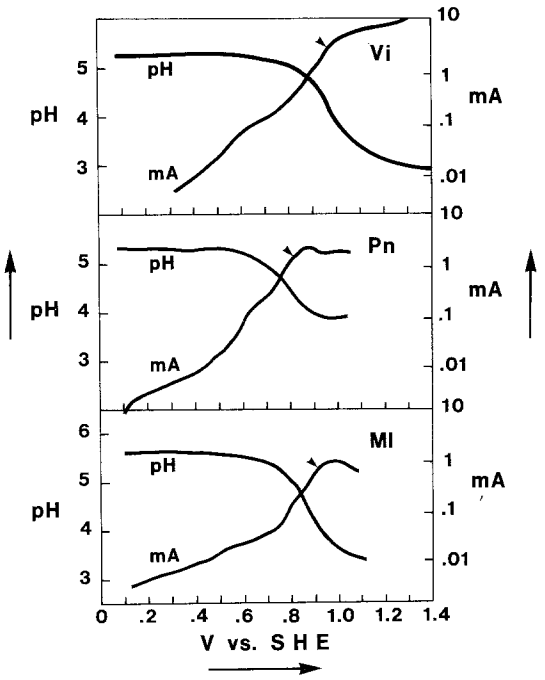

Fig. 8. Anodic leaching of violarite pentlandite and millerite in 0.1 mol dm^{-3} $NaNO_3$ as the potential is increased at 5 mV s^{-1}, showing the associated decrease in pH and increase in current. Arrow shows where the effect of sulphur forming on the electrode was first noticed.

3.3. *Similarity between violarite and pentlandite*

Both violarite and pentlandite have cubic-close-packed sulphur lattices, with the main structural differences being in the manner in which the nickel and iron atoms are arranged in the tetrahedral and octahedral sites within the sulphur lattice. Thus, there is very little difference between the atomic arrangement in the surface of a violarite or pentlandite crystal, and pentlandite and violarite crystal surfaces depleted in metal atoms or enriched in sulphur would be very similar. Thus the electrochemical properties of the mineral/electrolyte interfaces for the two minerals are also very similar. At lower pH values violarite does appear to undergo a form of near-reversible reaction near its rest potential, whereas the pentlandite appears to be more stabilized by some form of polarization. This is shown by a comparison of the IGP data for pH 0, 2, and 4 at currents of 0.01 mA cm^{-2}, shown in Figs. 2 and 3.

The potentials of the various proposed reactions have been transformed from the cyclic voltammetry and IGP data for Figs. 2 and 3 to a potential/pH diagram of Fig. 9 which is to be compared with the relevant portion of the E_h/pH diagram of Fig. 6c. The E_h/pH data from natural mineral assemblages already reported [8] are included on Figs. 9 and 6c to show how these data coincide with the passive potentials for pentlandite and violarite, and are very near to where the mineral surface can be enriched in either sulphur or metals. The rest potentials are the region where part of the metal at the surface of the sulphide has been leached out, and thus the surface can be regarded as partly enriched in sulphur. The areas shown as metal-rich surface or sulphur-rich surface indicate conditions where the surface of the mineral would essentially become all metal or all sulphur, respectively. Both violarite and pentlandite show some form of discontinuity at about pH 4. The thermodynamic diagram of Fig. 6c describes the equilibrium relations of the bulk minerals, and cannot be expected to correlate well with what are essentially diagrams of the reactivity of the mineral/electrolyte interfaces. For there to be any similarity, there would hve to be rapid diffusion between the solid bulk of the mineral and the surface where the reactions take place. Solid-state diffusion at these temperatures (25° C) could not be expected to keep pace with changes that take place at the crystal/electrolyte interface in the experimental situation, but geological time may allow the mineral crystal composition to equilibrate with the surface (see section 3.5).

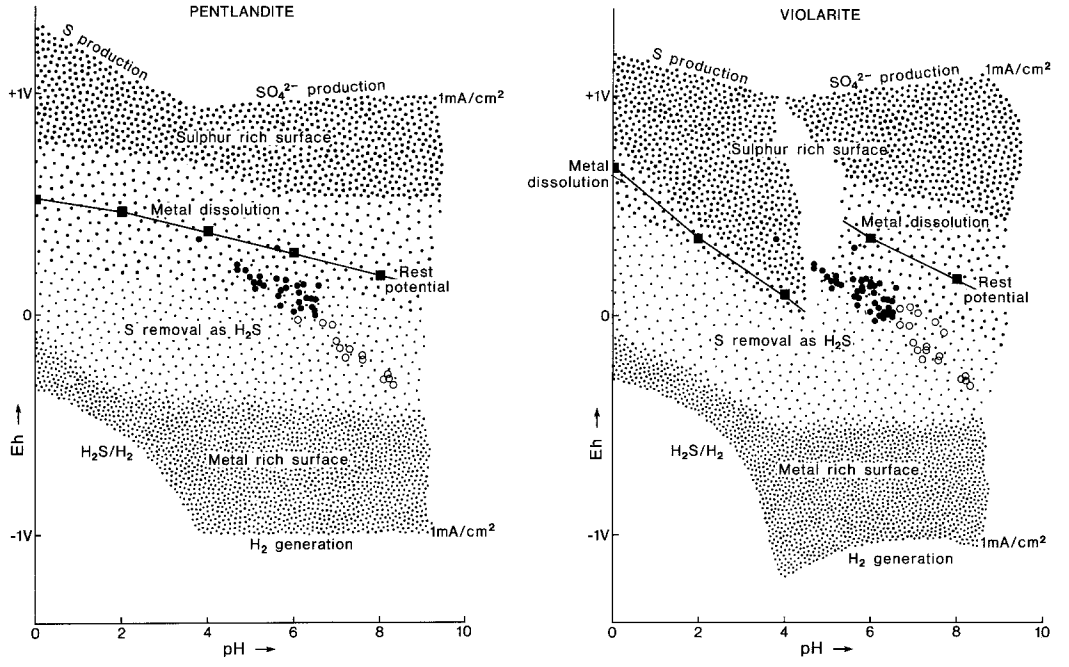

Fig. 9. Potential–pH diagrams for pentlandite and violarite, compiled from the IGP and cyclic voltammetry data. Data points are E_h–pH measurements made on pentlandite–violarite assemblages [8].

3.4. *Hydrometallurgical implications*

Figure 9 summarizes how conditions of pH and potential are critical to the surface properties of pentlandite and violarite, and thus they must have a controlling effect on flotation and leaching processes. In flotation, the mineral surface must be sufficiently metallic in nature for the xanthate-type collectors to be oxidized to a dixanthate on the surface so that it can be rendered hydrophobic [16]. Also, the release of nickel into the flotation baths by leaching processes can cause precipitation of xanthate. It is likely that nickel sulphides stored under conditions where they were passivated in the region of a metal-rich surface (Fig. 9a and b) would give better results in flotation than allowing the oxidation potential to rise sufficiently for metals to be leached and form oxide + oxyhydroxide coatings. Allowing the pH to fall would favour sulphur to form on the surfaces and either way a non-metallic surface would not favour the dixanthogen/xanthate reaction needed in flotation.

Acid leaching of pentlandite and violarite should be possible at low temperatures if some means could be devised whereby the potential of the sulphides could be made alternately oxidizing and reducing so that metal could be removed as M^{2+} and excess sulphur dissolved as H_2S. Acid leaching of pyrrhotite and millerite have already been studied from an electrochemical point of view [17]. The behaviour of violarite would be very similar to hexagonal pyrrhotite (Fe_9S_{10}), and the pentlandite more similar to millerite.

3.5. *Geochemical weathering of sulphides*

Geochemical weathering of pentlandite and violarite proceeds very slowly and there is sufficient time for solid-state diffusion to be able to keep in better pace with the faster processes at the interface. No data exist for the diffusion of metals in pentlandite or violarite, but if a comparison is made with pyrrhotite ($Fe_{1-x}S$), the data of Condit and Birchenall [18] can be extrapolated to give a value of about 10^{-17} cm^2 s^{-1} for the diffusion coefficient D at 298 K. Fick's Law states that where J is the number of moles of

$$J = -D(dc/dx)$$

metal passing through 1 cm^2 of mineral surface in 1 s, and dc/dx is the metal concentration gradient perpendicular to the mineral-electrolyte interface. If it is assumed that there is a change of metal concentration of 0.01 mol cm^{-3} over 10 nm to give what is probably an excessive concentration gradient, then $J \approx 10^{-13}$ mol cm^{-2} s^{-1}. Each divalent metal carries 2 positive charges, so this represents a current of $2JF$,

i.e., about 2×10^{-8} A cm^{-2}.

The smallest currents measured in the experiments reported here were 10^{-5} A cm^{-2}, some 500 times greater than the estimated solid-state diffusion rate. The solid-state diffusion currents flowing for geological time being much lower would require much less overpotential than those used in the electrochemical experiments; however, the actual geological stability fields of pentlandite and violarite may be more truly represented as lying within the more sparsely speckled regions of Fig. 9a and b. The pH of the environment where pentlandite is reacting to violarite is most likely to be between 7 and 8.5 [8], and at this pH range the measurements show that the oxidation potential would only have to rise to near − 0.3 V versus SHE to give sulphur excess at the surface of a pentlandite crystal, which would begin the growth of violarite. For violarite to react slowly to an oxide material at pH 5–6 [8], a higher oxidation potential of somewhere above zero to + 0.2 V versus SHE would give the required slight overpotential needed to allow violarite to weather to the oxide gossan minerals.

4. Conclusions

The mineralogical observations on sulphide minerals have led to a better understanding of the phase relationships of pentlandite, violarite, pyrrhotite, pyrite and sulphur, with sulphate and H_2S in solution. Electrochemical measurements indicate that, for violarite and pentlandite, the solution–mineral interfaces behave similarly and these results have been plotted within co-ordinates of E_h and pH so that the measured reactivity of these minerals can be compared with their thermodynamic stability. This approach can give insight into conditions needed for slow geological weathering of sulphide ores and is also applicable to understanding of mechanisms of the more rapid reactions used in hydrometallurgical leaching of sulphide minerals.

References

[1] E. H. Nickel, J. R. Ross and M. R. Thornber, *Econ. Geol.* 69 (1974) 93.
[2] E. H. Nickel, P. D. Allchurch, M. G. Mason and J. R. Wilmshurst, *ibid.* 72 (1977) 184.
[3] R. A. Keele and E. H. Nickel, *ibid.* 69 (1974) 1102.
[4] J. O'M. Bockris and A. K. N. Reddy, 'Modern Electrochemistry', Plenum Press, New York (1970).
[5] J. R. Craig, *Amer. Mineralogist* 56 (1971) 1303.
[6] J. Horvath and L. Hackl, *Corros. Sci.* 5 (1965) 525.
[7] M. R. Thornber, *Chem. Geol.* 15 (1975) 1.
[8] *Idem, ibid.* 15 (1975) 117.
[9] E. Peters, 'International Symposium on Hydrometallurgy' Chicago (edited by D. J. I. Evans and R. S. Shoemaker) American Institute of Mining, Metallurgical and Petroleum Engineering Inc. New York (1973) p. 205.
[10] J. R. Craig and A. J. Naldrett, 'GAC–MAC Conference' Sudbury (1971) 16.
[11] P. Toulman and P. B. Barton, *Geochem. et Cosmochem. Acta* 28 (1964) 641.
[12] D. D. Wagman, W. H. Evans, V. B. Parker, I. Halow, S. M. Bailey and R. H. Schumm, 'National Bureau of Standards (U.S.) Technical Note' 270–4 (1969).
[13] V. Rajamani and C. T. Prewitt, *Amer. Mineralogist* 60 (1975) 39.
[14] C. E. G. Bennett and J. Graham, *ibid.* 65 (1980) 800.
[15] L. F. Power and H. A. Fine, *Minerals Sci. Engng.* 8 (1976) 106.
[16] R. Woods, *J. Phys. Chem.* 75 (1971) 354.
[17] P. D. Scott and M. H. Nicol, 'Trends in Electrochemistry' (edited by J. O'M. Bockris, D. A. J. Rand and B. J. Welch) Plenum, New York, London (1976) 303.
[18] H. Condit and C. E. Birchenall, 'U.S. Department Com. Office Tech. Serv.' PB Rept. 147, 772 (1960) p. 85.